Distribution and Motion of Trifluoromethanesulfonate Anions in Poly(*p*-hydroxystyrene) and Polystyrene Films Studied by Multiple-Quantum NMR

Scott J. Limb, Bruce E. Scruggs, and Karen K. Gleason*

Department of Chemical Engineering, Massachusetts Institute of Technology, Cambridge, Massachusetts 02139

Received December 3, 1992; Revised Manuscript Received April 16, 1993

ABSTRACT: The degree of ammonium trifluoromethanesulfonate (triflate) salt aggregation in polystyrene (PS) and poly(*p*-hydroxystyrene) (PHOST) films was quantified using ^{19}F multiple-quantum (MQ) nuclear magnetic resonance (NMR) spectroscopy. The dispersion and diffusivity of photosensitizers containing triflate anions in polymer thin films affect the performance of chemical amplification resists. A low salt loading in PHOST films produced predominately dispersed anions, while both dispersed anions and salt aggregates coexist in films with higher loadings. In three films with high salt loadings, the maximum dispersed salt in PHOST films is 9.1 ± 2.0% w/w. The 10% w/w triflate salt in PS film has an aggregate fraction of 0.13 as compared to 0.29 for the same salt loading in PHOST. However, the 8.7 ± 2.0% w/w dispersed salt in this PS film falls within the range observed for the remaining PHOST films. In addition, the dispersed anions are less rotationally hindered in the PS film than in the PHOST films. In the PHOST films as well as the bulk triflate salt, oscillations are observed in the zero and two quantum intensities, indicating that the anions do not rotate isotropically at room temperature. These oscillations are absent in the PS film, indicating isotropic motion of the anion. An interaction between the salt anion and hydroxyl groups in PHOST could account for the rotation hindrance observed in the PHOST films, while its absence in PS would allows the anion to rotate isotropically. These differences in salt dispersion and mobility correspond to the observed variation in the T_g upon salt addition. A large plasticization effect (−23 °C) is observed in PHOST. The specific interaction between the salt anion and the hydroxyl group in PHOST may influence its free volume, configuration entropy, the degree of hydrogen bonding between the polymer chains, and degree of aggregate formation. Lack of such an interaction in PS may result in improved packing on the molecular level, corresponding to the observation of a small degree of antiplasticization (+5 °C). Finally, the growth rate of the higher order MQ coherences indicates that the salt aggregates in both types of films have interanion spacings similar to the bulk salt.

Introduction

Mixtures of photosensitive salts in thin polymeric films are used as chemical amplification resists. The sensitivity and resolution of these resists make them interesting candidates for advanced lithographic applications.[1-6] Upon irradiation, the photosensitive salt is converted to a strong acid, which reacts catalytically with the polymer to alter its solubility. A specific example is the acid-catalyzed reaction of poly[[(*tert*-butoxycarbonyl)oxy]styrene] to poly(*p*-hydroxystyrene) (PHOST).[5] The sensitivity of these resist systems has been related to the salt distribution in the polymer film.[7,8] Thus, it is desirable to quantify the distribution of photoactive salt in the polymer matrix. Because polystyrene (PS) derivatives are important components of some chemical amplification resist systems, PS and PHOST matrices will be investigated here.

Some early amplification resists were based on photosensitive onium salts having hexafluoroarsenate (AsF_6^-) or hexafluoroantimonate (SbF_6^-) anions.[5] The strong photoacids generated from these anions are subject to poisoning by organic vapors, degrading resist performance.[9] In addition, these materials raise concerns regarding heavy-metal contamination of electronic devices[10] and safe disposal of waste in the environment. More recently, photosensitive salts have been developed which contain trifluoromethanesulfonate (triflate) anions, thus eliminating the use of a heavy metal.[11-14] Upon exposure, this anion is converted to triflic acid, a weaker photoacid than those produced by the heavy-metal salts, and hence is less susceptible to organic vapor poisoning. Also upon exposure, the photosensitive cation is destroyed. Here, because it was much easier to obtain, the nonphotosensitive salt, ammonium trifluoromethanesulfonate ($NH_4^+CF_3SO_3$) will be used to examine the dispersion of the $CF_3SO_3^-$ anion in polymeric films by multiple-quantum (MQ) nuclear magnetic resonance (NMR).

The distribution of photosensitive salts in polymeric matrixes has been studied by a variety of techniques, including differential scanning calorimetry, scanning electron microscopy, and infrared spectroscopy.[8,15] In addition, MQ-NMR spectroscopy is able to characterize this dispersion on length scales <20 Å by probing the extent of the ^{19}F dipole–dipole coupling network.[15] When the salt is dispersed, the size of this network is small, while aggregated salt gives rise to large network sizes. In addition, the ^{19}F MQ-NMR signal arises only from the fluorine-containing salt, for which distribution information is sought, while no background signal arises from the polymer matrix, which comprises the majority of the sample. Finally, NMR requires only low-energy radio-frequency radiation, which is nondestructive to the photosensitive compounds used in chemically amplified resists, unlike the higher energy irradiation employed by X-ray diffraction and electron microscopies.

In the only previous MQ-NMR investigation of salt/polymer mixtures, only two general classes of behaviors were reported.[13] The salt was either almost completely dispersed in a poly(methyl methacrylate) matrix or predominately clustered in aggregates >20 Å in dimension in a poly(butyl methacrylate) matrix. Here, a method will be developed for using MQ NMR to quantify the degree of aggregation in mixtures having intermediate salt solubility in the polymer.

* Author to whom correspondence should be addressed.

0024-9297/93/2226-3750$04.00/0

Theory

MQ coherences develop only among strongly dipolar-coupled ^{19}F nuclei.[15] The order n of a MQ coherence is defined as the difference in z-magnetization between the initial and final states of the nuclei. The highest MQ order which can be achieved is simply equal to the number of dipolar-coupled nuclei. Since the magnitudes of the dipolar coupling constants vary inversely with the cube of internuclear distance, MQ NMR only probes clustering over distances of several bond lengths.

A statistical model has been used to describe the intensity distribution among the various MQ orders.[17-20] In the statistical limit, the total intensity of an n-order coherence, $I_n(\tau)$, is directly related to the number of ways of achieving that coherence among the N dipolar-coupled nuclei. For $N > 6$, a Gaussian intensity distribution is obtained.

$$I_n \propto \exp[-n^2/N] \quad (1)$$

Equation 1 applies strictly only to isolated groups of N nuclei at long preparation times, τ. However, many large dipolar-coupled spin networks display Gaussian MQ intensity distributions at values of τ such that $N(\tau) < 70$. Thus, $N(\tau)$, the effective number of dipolar-coupled spins, will be obtained from a least-squares fit to the experimental intensity distribution to eq 1 at each τ.

In this paper, the sum of the n quantum intensities, I_n, for $-16 \le n \le 16$, at a fixed τ is normalized to 1. Since the MQ intensity distribution is symmetric, $I_n = I_{-n}$ (eq 1), the intensity of the nonzero orders will be reported as $I_{|n|}$, where $I_{|n|} = I_n + I_{-n}$. This allows visual conformation of the normalization criteria when all the intensities are graphed. As will be discussed in the Experimental Section, only even-order coherences are excited by the experiment used in this work. Also, the differences between populations and true 0Q coherences are not resolved in this experiment. An example of populations being detected at the 0Q intensity position can be seen in the spectra of isotropically rotating and dispersed AsF_6^- anions, well dispersed in poly(methyl methacrylate).[15]

When the number of coupled spins is small, nonstatistical behavior is often observed.[21,22] Oscillations in MQ coherence intensity dynamics are signatures of strong dipolar couplings among a small number of spins. A small group of nuclei will have only a few unique frequencies associated with its dipolar coupling network. As a result, distinct oscillations in the MQ coherence intensities with preparation time, τ, occur. Networks with larger numbers of dipolar-coupled nuclei have many more characteristic dipolar frequencies leading to destructive interference of the oscillations.

Oscillatory behavior might be anticipated for the MQ intensities arising from the three ^{19}F nuclei on an isolated $CF_3SO_3^-$ anion. As the individual anions are placed closer together, or even close-packed in salt aggregates, the intermolecular ^{19}F–^{19}F dipolar couplings will increase and the oscillations in MQ intensities will destructively interfere. The allowed MQ orders for an isolated CF_3 would have $|n| \le 3$. Thus, when only even-order coherences are excited, only the 0Q and |2|Q intensities are allowed. Furthermore, the sum of these two intensities must be conserved.

Molecular motion acts to reduce the average magnitude of the dipolar couplings. For example, the highly symmetric AsF_6^- and SbF_6^- anions examined previously[14] rotate isotropically at temperatures above 150 K. Such isotropic motion averages the intramolecular ^{19}F–^{19}F dipolar couplings to zero. However, lack of translational motion preserves the intermolecular dipolar couplings, allowing MQ coherences to be created. Thus, all correlations arise from interion couplings and thus are a direct probe of salt dispersion. In contrast, the trifluoromethanesulfonate anion, under study here, is capable of anisotropic motion. While this type of motion serves to reduce the magnitude of the intramolecular dipolar coupling, the average maintains a nonzero value. This difference should introduce unique features into the ^{19}F MQ coherence development of the ammonium trifluoromethanesulfonate.

Experimental Section

The polymers, PHOST and PS, were obtained from secondary standard stock of Polyscience while the salt, ammonium trifluoromethanesulfonate, was obtained from Aldrich. Since this salt is hygroscopic, the 200-mg bulk salt sample was prepared under nitrogen. Films were solvent cast from a 6% w/w polymer in tetrahydrofuran solutions having either 2%, 10%, 20%, or 30% w/w salt in PHOST or 10% w/w salt in PS and air dried for 1 day. In order to remove residual solvent, the films were then vacuum dried at 60 °C for 48 h. The resulting NMR samples of the polymer films contained between 5 and 70 mg of salt.

Two PHOST samples, pure and 10% w/w salt, were characterized with differential thermal analysis (DTA) at a heating rate of 15 °C/min using a Seiko TG/DTA-320 instrument. Differential scanning calorimetry (DSC) performed using a heating rate of 10 °C/min on a Perkin-Elmer DSC-7 was used to analyze the pure and 10% w/w salt PS samples. In all experiments, T_g was taken as the heating inflection's midpoint.

All NMR spectra were taken at room temperature on a home-built spectrometer having a 280-MHz ^{19}F Larmor frequency. A delay of 40 s, greater than 5 times the spin–lattice relaxation of the bulk salt, allowed the sample's magnetization to return to equilibrium between signal acquisitions. The MQ NMR spectroscopy was performed using the H_{yx} two-quantum propagator.[16] The length of 90° pulses was 1.6 μs, while the overall 8-pulse sequence cycle time was set at 31.2 μs. The phase of the preparation period pulses was shifted with respect to the mixing period pulses by increments of 5.6°, allowing detection of n quantum coherences with $|n| \le 16$. A 1-ms delay following the mixing period allowed for the decay of transverse magnetization prior to the 90° detection pulse used to detect the stored z-component of the magnetization. Spin locking with periodic sampling during the detection period was employed to further enhance the signal-to-noise ratio.[18]

Results and Discussion

The Fourier-transformed free-induction-decay (FID) spectra, normalized to the same peak height, of the salt in bulk form and at 10% loadings in the PS and in PHOST films are displayed in Figure 1. The corresponding best single Lorentzian fit to each spectra is also shown. The Lorentzian character of each line shape is indicative of partial motional averaging of the dipolar couplings in the samples.[24] Couplings which are static on the time scale of the NMR experiment generally give rise to Gaussian line shapes. The spectrum for the PHOST sample is slightly narrower than that for the bulk salt. The full width at half-maxima (fwhm) corresponding to the remaining PHOST samples (Table I) are also quite similar to those of the bulk salt. However, for the PS sample, the spectrum has narrowed significantly.

Both ^{19}F–^{19}F and ^{1}H–^{19}F dipolar couplings contribute to the observed line widths of the FID spectra. Other factors such as chemical shift anisotropy can produce broadening as well. Since dipolar couplings vary as the inverse cube of the internuclear distance, the degree of salt aggregation should strongly affect the magnitude of the ^{19}F–^{19}F intermolecular couplings. The square root of the second moment due to dipolar interaction, $M_2^{1/2}$, can be related to internuclear spacings through the van Vleck

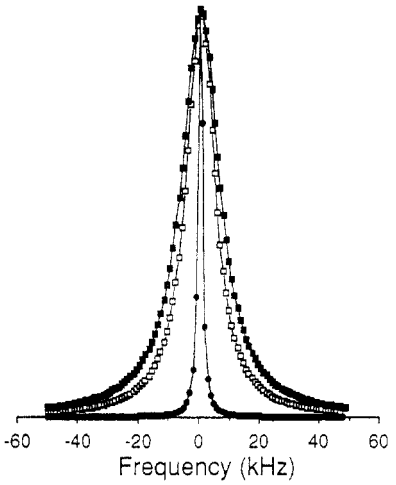

Figure 1. Fourier-transformed free-induction-decay ^{19}F NMR spectra of the bulk triflate salt (solid squares) and of the PHOST (open squares) and PS (solid circles) films containing 10% w/w triflate salt. The solid lines represent the best-fit Lorentzian to each spectrum. Differences in line width arise from changes in interanion spacing and/or reorientation of the anion itself.

Table I. NMR Line Widths (fwhm's) for Ammonium Trifluoromethanesulfonate in Bulk and at Various % w/w in Polymer Films

sample	fwhm (kHz)	sample	fwhm (kHz)
bulk salt	15.0	10% in PHOST	11.3
10% in PS	2.0	20% in PHOST	12.6
2% in PHOST	12.8	30% in PHOST	10.8

equation.[23] A Lorentzian line shape truncated at a bandwidth of π times the fwhm yields a value of $M_2^{1/2}$ equal to the fwhm.[24] Dispersed anion pairs at spacings >10 Å will have intermolecular couplings which contribute <0.13 kHz to the $M_2^{1/2}$ of the line shape. Alternatively, if ions of the bulk salt are uniformly arranged on a cubic lattice corresponding to a salt density of 1.80 g/cm^3, intermolecular ^{19}F–^{19}F couplings lead to a $M_2^{1/2}$ of 2.71 kHz. In addition, intramolecular couplings can vary between samples. The $M_2^{1/2}$ calculated by the van Vleck equation for a static CF_3 group is 9.7 kHz. If the CF_3 group rotates rapidly about its C_3 axis without any other reorientation of the anion, this value is scaled by $^1/_4$,[25] corresponding to an $M_2^{1/2}$ of 2.4 kHz. Additional motion of the CF_3 group would reduce the second moment even further, with rapid isotropic motion yielding a zero value.

The observed $M_2^{1/2}$ values for the bulk salt or at any loading of salt in PHOST indicate static or anisotropically rotating CF_3 is potentially present (Table I). However, comparison to other compounds containing the CF_3 moiety indicates that anisotropic rotation is more likely at room temperature.[26] Finally, the smaller $M_2^{1/2}$ of the line shape for the 10% salt loading in PS most likely indicates additional motion of the anion. Similarly, the ^1H–^{19}F interactions can vary between samples depending on average spacings and the degree of motion. Such interactions can dominate the spectra, obscuring variations in ^{19}F–^{19}F intramolecular couplings. This was the case in a previous study of triphenylsulfonium metal fluoride salts in poly(methyl methacrylate) and poly(*n*-butyl methacrylate).[15] By contrast, significant changes in the line width between the spectra of the salt in different polymers and in bulk form are observed here. Unfortunately, the source of these changes cannot be uniquely identified based on the FID spectra alone.

The evolution of the MQ coherence intensities with preparation time, τ, provides further insight into the degree of aggregation and mobility of the anions in the polymer

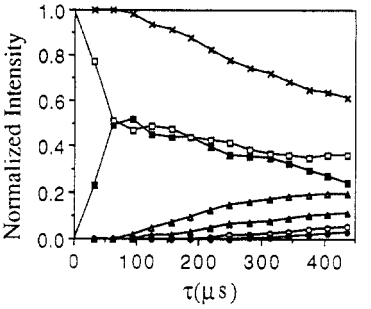

Figure 2. Normalized even-order MQ coherence intensities for the 98% pure triflate salt at room temperature as a function of preparation time, τ. The solid lines simply connect the data points for each order: 0Q (open squares), |2|Q (solid squares), |4|Q (open triangles), |6|Q (solid circles), |8|Q (open circles), |10|Q (solid diamonds), and the sum of 0Q+|2|Q (solid triangles). Oscillations in 0Q and |2|Q arise from strong dipolar couplings with the CF_3 group of a single anion. The sum of the 0Q and |2|Q intensities produces destructive interference of these oscillations. Orders with $n \geq 4$ grow in monotonically and result from interion couplings. The intensities of orders with $n \geq 4$ follow a Gaussian distribution and define an effective number of correlated ^{19}F nuclei, $N(\tau)$ (eq 1).

film samples. Simplification is achieved since the MQ coherence intensities develop only through ^{19}F–^{19}F dipolar couplings, as ^1H–^{19}F couplings are averaged to zero under the MQ propagator, H_{yx}.[20] The even-order coherence intensities produced by this propagator as a function of τ for the bulk triflate salt can be seen in Figure 2. Initially, all the intensity from the bulk triflate salt is in the 0Q order, but the |2|Q coherences grow in rapidly at small τ. Even-order intensities having $|n| \leq 10$ are displayed in Figure 2. Although not displayed, significant intensity with respect to the noise is observed up to the |16|Q order at long τ, indicating a large dipolar-coupled network. Neither the decay of the 0Q nor the growth of the |2|Q is monotonic. Rather, small oscillations are observed, suggesting that a small group of spins is more strongly coupled to each other than to the remaining nuclei in the lattice. However, taking the sum of these two intensities does yield a monotonic decay. These observations can be accounted for if the dipolar couplings within the CF_3 group of an individual anion are large with respect to interion ^{19}F–^{19}F dipolar couplings. The growth of the higher order coherences also occurs without oscillation. This suggests the coherences with $|n| \geq 4$ arise from a large number of nuclei which have been correlated through their dipolar couplings.

Figure 3 shows $N(\tau)$ versus τ for the bulk salt when $N(\tau) \geq 6$. As in previous studies,[15,17-20] these $N(\tau)$ values were obtained using only the intensities of the positive orders in a least-squares fit to eq 1. The solid line in Figure 3 represents the best fit to empirical equation $N(\tau) = N_\beta \exp(\beta M_2^{1/4} \tau^{1/2})$, where N_β and β are constants. This equation has provided a good description of the MQ growth curves of several other ^{19}F-containing salts using $N_\beta = 0.53 \pm 0.18$ and $\beta = 3.7 \pm 0.5$.[20] For Figure 3, the best-fit value of N_β is 0.55, which agrees well with the previous work. The best-fit value of $\beta M_2^{1/4}$ is 204 s$^{-1/2}$, yielding an $M_2^{1/2}$ range for the homonuclear ^{19}F–^{19}F coupling of 3.21 ± 0.85 kHz using the previously observed range for β. As expected, this value of $M_2^{1/2}$ is smaller than that obtained from the FID spectra, which contains the effects of heteronuclear couplings as well. However, $M_2^{1/2}$ for interanion couplings of 2.71 kHz for a cubic lattice of the bulk salt falls in the range determined by the NMR experiment. Intraion couplings will increase $M_2^{1/2}$ further. However, a static anion would increase this value above the upper limit of this range. Thus, some degree

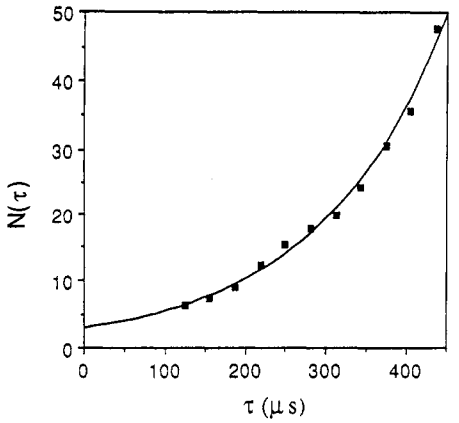

Figure 3. $N(\tau)$ values for the bulk triflate salt obtained from the data of Figure 2, showing the monotonic increase to >45 effectively coupled ^{19}F as τ is increased. The solid line is the best fit to an empirical equation which can be used to estimate the average dipolar field due only to homonuclear ^{19}F couplings.

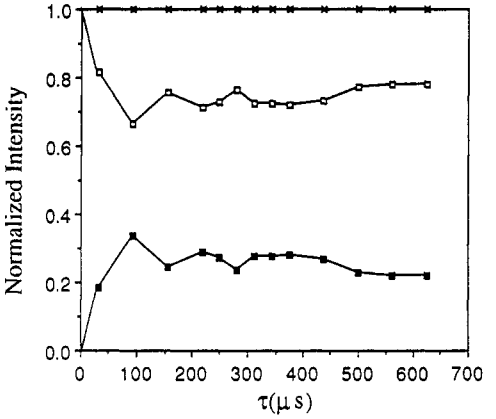

Figure 4. Normalized even-order MQ coherence intensities for the 2% w/w pure salt in PHS as a function of τ. Solid lines connect the intensities for 0Q (open squares), |2|Q (solid squares), and the sum of 0Q+|2|Q (solid triangles). Pronounced oscillations in 0Q and |2|Q and their destructive interference indicate strong couplings among the three ^{19}F nuclei on each anion and that the majority of the anions are well dispersed in the polymeric matrix. Orders with $n \geq 4$ are absent since least n dipolar-coupled spin-$^1/_2$ nuclei are required to create an n-quantum coherence.

of anionic motion is likely in the bulk salt, in agreement with the observation of a Lorentzian FID line shape.

The MQ intensity spectra of the 2% salt loading in PHOST (Figure 4) show only 0Q and |2|Q intensities. The lack of higher order coherences as compared to the bulk salt indicates a change in anion spacing, since only even-order coherences having $|n| \leq N$, the number of coupled spins, can be observed. Thus, the presence of only 0Q and |2|Q coherences suggests the vast majority of the $CF_3SO_3^-$ anions are well dispersed in the PHOST matrix. Intraion dipolar interactions would then be much more significant than interion ones, forming nearly isolated groups of three coupled ^{19}F nuclei. Note that the oscillation pattern in the 0Q and |2|Q coherences at early τ matches that of the bulk salt at early times, confirming the importance of the intraion couplings for producing these features in the bulk salt. At longer times, these oscillations destructively interfere in the bulk salt as a result of the correlations between anions. The nonzero intensity in the |2|Q coherence also indicates a static or anisotropically reorienting anion, most likely due to rotation about the C_3 axis. Rapid isotropic rotation is ruled out, since this would average the intramolecular dipolar coupling to zero, and no |2|Q coherence would be observed. Thus, the MQ results at a 2% loading indicate that the salt is predominately dipsersed in the PHOST matrix, and anion motion, if any, is anisotropic.

At higher salt loadings in PHOST, the MQ coherence intensity development appears to be a superposition of that of the pure salt (Gaussian intensity distribution for all even orders) and that of the 2% salt loading in PHOST (0Q and |2|Q intensities only). Thus, in these remaining PHOST samples, some of the salt appears to be aggregated while the rest is dispersed. As the salt loading increases, the intensities corresponding to the Gaussian distribution increase relative to the 0Q and |2|Q intensities. Thus, as might be anticipated, the fraction of salt in the aggregated form appears to be increasing with salt loading. For the salt/polymer films, which are expected to contain both aggregates and dispersed anions, non-Gaussian intensity is expected in the 2Q intensity. The values of $N(\tau)$, the effective number of correlated spins associated with the aggregates, are calculated from variance of the Gaussian fit to eq 1 for the orders $n \geq 4$. The 2Q intensity is not used in this case since some of its intensity is attributable to the isolated anions. The calculated values of $N(\tau)$ for the salt/polymer mixtures are comparable to the values for the pure salt at the same preparation time. This indicates that both the interion spacing and anion motion in the aggregates is similar to that of the pure salt.

Like the bulk salt, the PS film with 10% w/w salt displays a Gaussian distribution of all the positive MQ intensities, yielding a similar value of the effective number of correlated spins, $N(\tau)$ at all τ. Thus, a portion of salt in this sample appears to be aggregated. However, the 0Q intensity is much greater in the PS mixture than in the bulk salt. If the isolated $CF_3SO_3^-$ anion in PS rotated, the average value of the intramolecular dipolar couplings could be significantly reduced, or, in the case of rapid isotropic rotation, averaged to zero. Thus, 0Q coherence would be created, but little or no 2Q coherence would develop. In the 10% PS sample, the large 0Q intensity most likely arises from the dispersed salt while the positive-order intensities arise predominately from the clustered anions. Furthermore, the reduced line width of FID spectra (Figure 1) of the 10% PS film is also consistent with enhanced molecular reorientation of the triflate anion in PS as compared to PHOST.

The difference in the mobility of the dispersed anion in the two polymer matrices may be related to the potential for specific interaction between the salt anion and hydroxyl groups in PHOST. Such an interaction could account for the rotation hindrance observed in the PHOST films, while its absence in PS would allow the anion to rotate isotropically. Although not probed directly, the translational motion of the anion in the two polymers may also differ. Different diffusivities of the photoacid generated from the salt would result which would affect the extent of catalytic reaction within the polymer.[27] As the polymeric matrix of a chemical amplification resist is converted to PHOST upon irradiation, an increased possibility for a specific interaction with the hydroxyl group on the polymer matrix may cause the diffusivity of the triflate anion to vary with the degree of irradiation.

Parts a–f of Figure 5 show the normalized intensities of various MQ orders for all samples. Initially, only 0Q intensity is present (Figure 5a) while 2Q and higher order coherences develop at progressively later times (Figure 5b–f). In all the PHOST samples, the decay of the 0Q and the growth of the |2|Q intensities exhibit oscillations. No oscillations are observed in the 0Q and |2|Q behavior of the PS film. The oscillations are clearest for the PHOST samples with the lowest salt loadings, 2% and 10%, which

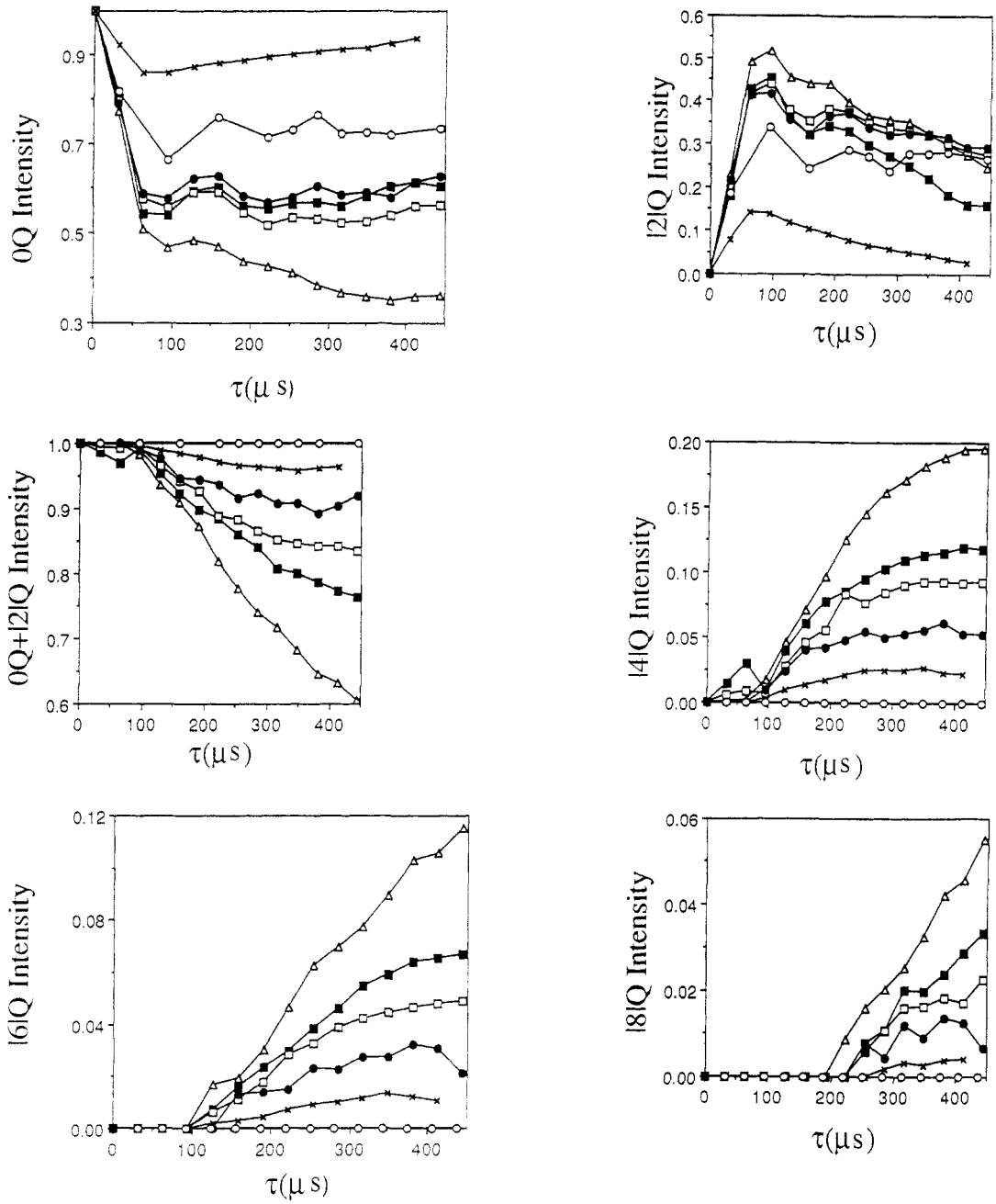

Figure 5. Normalized MQ coherence intensities as a function of τ for the bulk triflate salt (open circles); four PHOST films with various wt % of the triflate salt; 2% (solid squares), 10% (solid circles), 20% (solid triangles), and 30% (solid diamonds); and the 10% triflate in PS film (open squares). The oscillations in the (a) 0Q and (b) 2Q intensities display more destructive interference as interion couplings increase at higher salt loadings until behavior similar to the bulk salt is achieved. Lack of oscillation for the PS sample most likely indicates increased mobility of the $CF_3SO_3^-$ anion. (c) The sum 0Q+|2|Q shows no oscillatory behavior as expected for a small number of coupled nuclei, such as a CF_3 group. The decay rates of this sum also show a clear trend with increasing salt loading. This simple trend is not apparent in the intensity data for either order alone. (d) |4|Q, (e) |6|Q, and (f) |8|Q show monotonic growth with τ. In these three graphs, faster growth rates are associated with higher salt loading in PHOST and the relative rates of the bulk salt and PS film samples are in the same order as the decay rates for the 0Q+|2|Q graph.

are expected to contain the highest fraction of dispersed anions. Destructive interference of these oscillations by the strong intermolecular ^{19}F–^{19}F dipolar couplings in salt aggregates can be observed at the higher salt loadings of 20% and 30% and in the bulk salt. In the case of an isolated CF_3 group, which produces only 0Q and |2|Q intensities, a decrease in the intensity of one order should lead to a increase in the other. Indeed, the local minima in the 0Q intensity correspond to local maxima in the |2|Q at ~95 and ~285 μs, and the addition of the 0Q and |2|Q signals (Figure 5c) results in a monotonic decay curve. Total lack of oscillation, such as in the 10% PS sample, indicates severely reduced intramolecular dipolar coupling, indicative of more extensive anion reorientation.

Examination of Figure 5c clearly indicates the ordering of the decay rates of the sum $(I_0+I_{|2|})$ for the various samples. The decay rate of the bulk salt is faster than those for any of the salt/polymer films. For the PHOST samples, the fastest rate is seen at the highest salt loading, 30%, followed in order of decreasing salt content by the 20%, 10%, and 2% samples. Note that, at the 2% loading in PHOST, only 0Q and |2|Q intensities are observed. Thus, the sum $(I_0+I_{|2|})$ does not decay at all. The 10% loading in PS yields a slower decay than the same loading in PHOST but is still faster than the 2% w/w PHOST film. The identical ordering of rates is seen for the growth of |4|Q, |6|Q, and |8|Q coherences in parts d–f of Figure 5, respectively. Note that the intensity of the |6|Q coherence

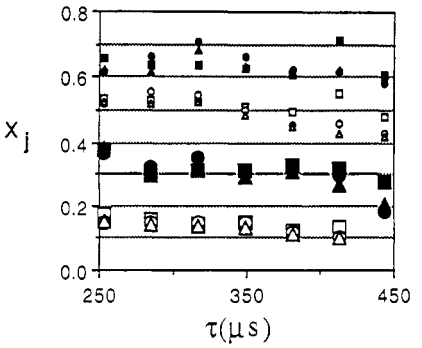

Figure 6. Fraction of $|n|$Q coherence arising from salt aggregates in the polymer films, $x_{|n|}$. Since this fraction is only a weak function of τ and the MQ order examined, the average value is taken as a measure of the fraction of salt in sample which is aggregated.

must be built from the lower order coherences and thus requires an induction time of ~100 μs. The |8|Q coherences require nearly twice as long to be created. Also, in accordance with the expected statistical distribution of MQ coherences (eq 1), the higher order coherences are less intense than lower order ones. Thus, only orders with $|n| \leq 8$ are displayed.

While variation in rates occurs, the curves in parts c–f of Figure 5 appear similar in shape, supporting the hypothesis that the observed intensities are a superposition of the signals arising from the aggregates and the dispersed salt. MQ intensity distributions from samples containing more than one characteristic spin correlation size have been considered as linear combinations of Gaussian distributions.[18,28] Here, rather than considering the distribution at a given τ as a whole, each MQ coherence intensity $I_{j,\text{film}}$ is considered separately. The subscript j represents either one particular $|n|$ quantum order or the sum of two such orders, and x_j is the fraction of salt in the aggregates. Thus, the signal detected for a given film will be a linear combination of the signal from aggregates, $I_{j,\text{agg}}$, and that from the dispersed salt, $I_{j,\text{disp}}$,

$$I_{j,\text{film}} = x_j I_{j,\text{agg}} + (1 - x_j) I_{j,\text{disp}} \quad (2)$$

At each τ, the aggregates and the bulk salt are observed to have approximately the same correlation size, $N(\tau)$. Therefore, $I_{j,\text{agg}}$ is taken to be equal to the measured intensities for the bulk salt, $I_{j,\text{salt}}$. The three dipolar-coupled nuclei of a disperse $CF_3SO_3^-$ anion can create only 0Q and |2|Q order coherences. Thus, when j represents the sum of the 0Q + |2|Q intensities, $I_{0+|2|,\text{disp}} = 1$, while $I_{|n|,\text{disp}} = 0$ for all $n \geq 4$. Substituting these relationships into eq 2 and solving for x_j yields

$$x_{0+|2|}(\tau) = \{1-[I_{0+|2|,\text{film}}(\tau)]\}/\{1-[I_{0+|2|,\text{salt}}(\tau)]\} \quad (3)$$

$$x_{|n|} = I_{|n|,\text{film}}(\tau)/I_{|n|,\text{salt}}(\tau): \quad |n| \geq 4 \quad (4)$$

By these definitions, $x_j = 1$ for the bulk salt and $x_j = 0$ for totally dispersed $CF_3SO_3^-$ anions at all values of n and τ. In between these two extremes, larger fractions correspond to a higher degree of salt aggregation in the polymer film. For a given film, the fractional intensity attributed to aggregates should be independent of the n-quantum order or the preparation time, τ, considered.

For each film, the intensity ratios, $x_{0+|2|}$, $x_{|4|}$, and $x_{|6|}$ at each value of τ, calculated by eqs 3 and 4, are plotted in Figure 6. Due to their weak signal levels, higher order ratios were not calculated. In agreement with the initial hypothesis, $x_{|n|}$ depends strongly on sample identity but only weakly on n or τ. Thus, x_j can be considered the fraction of salt aggregated in the film. For the 10% w/w triflate salt in PHOST, $x_j = 0.29 \pm 0.05$ (Figure 6). As might be expected, at higher salt loadings in the PHOST films, x_j increases. The average values of x_j for the 20% and 30% w/w salt in PHOST are 0.49 and 0.63, respectively. Thus, the fraction of the salt residing in aggregates can be quantified through analysis of the MQ-NMR intensities.

Table II. Glass Transition Temperatures (°C)

	PHOST	PS
(a) bulk polymer	153	101
(b) 10% w/w salt/polymer	130	106
(c) difference (b – a)	–23	5

If the triflate salt has a maximum solubility in PHOST at room temperature, the product of the salt loading and the degree of dispersion ($1-x_{|n|}$) should be constant. For the 10, 20, and 30% salt loadings these products are 7.1, 10.2, and 1.1% w/w salt in PHOST. The differences between these numbers may be a reflection that these solvent-cast films are not necessarily at thermodynamic equilibrium. Kinetic limitations during film formation from the solvent mixture may also be important in determining the degree of salt dispersion.[29] Gradients in dispersed salt concentration may also exist. Poor solubility of onium salts in the polymers has been suggested to cause salt movement away from the drying interface and into the bulk film, which still contains a high concentration of solvent.[30] Still, the overall agreement of these values provides an estimate for the maximum salt loading that can be dispersed. At salt loadings less than the maximum solubility, total dispersion of the salt is anticipated. Indeed, the 2% w/w PHOST sample, having a lower salt loading than calculated solubility range, contains only dispersed salt.

The average value of x_j for a salt loading of 10% in PS is 0.13, indicating that only a small fraction of the salt is aggregated. Thus, the average x_j value for PS is lower than that for PHOST at the same 10% salt loading. However, multiplying the salt loading by $1-x_j$ yields 8.7% w/w dispersed salt in PS, within the same range as for the PHOST films. Thus, further work is required to determine if the solubility of triflate in PS is greater than that in PHOST.

Besides differences in dispersed anion mobility, the change in glass transition temperatures (T_g) upon adding 10% w/w salt to the pure polymer is of opposite sign for the two polymers (Table II). Our T_g measurements of the pure polymers, 153 and 101 °C, are consistent with literature data and fall within the manufacture's specified ranges for PHOST[30] and PS,[31] respectively. In PHOST, where rotational hindrance of the anion was observed by NMR, the salt has a strong plasticizing effect, producing a T_g by 23 °C lower than that of the pure sample. At the same salt loading, a small degree of antiplasticization is observed in the PS film, resulting in a 5 °C rise in T_g over that of pure PS. Recall that the dispersed anion undergoes isotropic rotation in PS. Thus, mobility differences of the dispersed triflate anions correlate to the observation of plasticization in PHOST and antiplasticization in PS.

Several factors previously proposed to affect plasticization and antiplasticization in other polymer/additive blends[32] are expected to be significant in determining the behavior of the triflate salt/polymer mixtures studied here. One consideration is the glass transition temperatures of the polymer and the additive. Since the same salt is used in both PS and PHOST, only the glass transition temperatures of the polymers need be considered here. In pure PS, in which T_g is more than 50 °C lower than the pure PHOST, fast (>12 kHz) isotropic rotation is observed.

By contrast, the dispersed anions in PHOST are rotationally hindered. Thus, greater anion mobility occurs where polymeric mobility is the highest, as indicated by a lower T_g. However, the NMR experiments are being carried out at room temperature, below the T_g of either polymer, and thus no large difference in polymeric mobility is expected. Another factor is the efficiency of molecular packing in the blend relative to the pure polymer.[33] Improved packing, associated with densification and loss of free volume, reduces polymeric mobility, thus increasing T_g. It is possible that when the dispersed salt is not constrained to interact with a specific site, it is able to pack more efficiently into void space in the polymeric matrix. This could contribute to the antiplasticization behavior observed for the PS film. Also, specific interactions between the polymer and the diluent can play an important role in determining the T_g of the mixture. In PHOST, the hydroxyl group may provide such a specific site for interaction with the triflate anion. This interaction would disrupt some interchain hydrogen bonds which occur between hydroxyl groups in pure PHOST, thus increasing chain mobility resulting in plasticization. Also, aggregation of additives generally increases the mobility of the polymer matrix leading to plasticization. Thus, the fraction of salt aggregates higher in 10% w/w salt in PHOST than in 10% w/w salt in PS could account for the plasticization effect in PHOST films. Interestingly, the salt is less mobile when acting as a plasticizer in PHOST than an antiplasticizer in PS. This is in contrast to reports on other polymer mixtures which indicate that enhanced mobility of the additive is associated with plasticization of the polymer.[34,35] Clearly, motion of the additive is only one of many influences of the T_g of the final mixtures. Thus, correlations between additive mobility and plasticization behavior are highly system specific.

Conclusions

The fraction of salt aggregation in polymer films can be quantified using multiple-quantum NMR spectroscopy. When both salt aggregates and dispersed anions coexist, the observed intensity for each MQ order was found to be a linear combination of signals from each environment. This eliminates the need to describe the intensities of the MQ orders by Gaussians and is of particular value when the experimental distribution is non-Gaussian. In addition, this behavior reveals that interanion spacing in the salt aggregates in both types of polymer films is similar to that in the bulk salt.

Poly(*p*-hydroxystyrene) (PHOST) films with high salt loadings: 10%, 20%, and 30% w/w salt; contained both dispersed anions and salt aggregates. The fraction of dispersed salt in these three samples was found to be 9.1 ± 2.0% w/w. At a lower salt loading of only 2% w/w, only dispersed anions were observed. The oscillations in the 0Q and |2|Q intensities with MQ preparation time indicate that the anions in the PHOST matrix and in the bulk salt are rotationally hindered at room temperature.

The 10% w/w triflate salt in PS also contains both dispersed and aggregated salt. However, this film differs from the corresponding PHOST sample in that the fraction of dispersed anions, 0.13, is less than the 0.29 fraction observe in 10% w/w salt in PHOST. However, the 8.7 ± 2% w/w dispersed salt in this PS film falls in the range observed for the other PHOST films with high salt loadings. In addition, isotropic rotation of the dispersed anions is observed in PS.

The differences in salt dispersion and mobility probed by MQ NMR were found to correspond to changes in T_g with salt addition. The higher degree of aggregation in PHOST may contribute to the large plasticization effect which is observed. In addition, the specific interaction between the hydroxyl group in PHOST and the triflate anion, as evidenced by the rotational hindrance of the anion, may promote aggregation and/or increased free volume. In addition, a specific interaction between the salt and the PHOST hydroxyl group could lead to decreased interchain hydrogen bonding and thus plasticization of the polymer chains. In PS, the interaction of the anion with a specific site is absent, allowing isotropic rotation of the triflate anion. In addition, the geometric constraint requiring the anion to be associated with a specific site on the polymeric unit is removed, and it is possible that molecular packing is improved, leading to the observed small anitplasticization effect.[32]

Salt dispersion is desired when designing a chemically amplified resist, correlating to increased sensitivity.[7,8] Previous work has shown that favorable interactions between the salt and more polar polymer matrices lead to improved dispersion of the photosensitive salt. However, in this work, a very specific favorable interaction of the polymer and the salt, that is, between the hydroxyl group of the PHOST and the triflate anion, appears not to increase dispersion. In these systems, other considerations, such as the T_g of the polymer matrix, the configuration entropy, and/or the free volume of the salt/polymer mixture, may become the dominant factors in determining the degree of dispersion achieved.

Finally, the difference in the mobility of the dispersed anion in the two polymer matrices caused by a specific interaction between the polymer and the salt could influence the performance of the chemically amplified resist. In this study, the interaction between the salt anion and hydroxyl groups in PHOST mostly likely accounts for the rotational hindrance of the anion observed in the PHOST films, while its absence in PS corresponds to the observation of isotropic anion rotation. This specific interaction may also effect translational motion of the anion. Triflate anion diffusivity could depend upon exposure in chemical amplification resists where PHOST is an irradiation product. Variation in diffusivity can then impact the extent of catalytic reaction within the polymer.

Acknowledgment. This work has been supported by National Science Foundation Grant No. CTS-9057119. The authors are grateful to Dr. David Lathrop for assistance with these experiments.

References and Notes

(1) Ito, H.; Willson, C. G. *ACS Symp. Proc. Ser.* **1984**, *242*, 11.
(2) Ito, H. *SPIE Proc.: Adv. Resist Technol. Process. V* **1988**, *920*, 33.
(3) O'Brien, M. J.; Crivello, J. V. *SPIE Proc.: Adv. Resist. Technol. Process. V* **1988**, *920*, 42.
(4) Tarascon, R. G.; Reichmanis, E.; Houlihan, F.; Shugard, A.; Thompson, L. F. *Polym. Eng. Sci.* **1989**, *29*, 850.
(5) Reck, B.; Allen, R. D.; Twieg, R. J.; Willson, C. G.; Matuszczak, S.; Stover, H. D. H.; Li, N. H.; Frechet, J. M. J. *Polym. Eng. Sci.* **1989**, *29*, 960.
(6) Lamola, A. A.; Szmanda, C. R.; Thackeray, J. W. *Solid State Technol.* **1991**, *34*, 53.
(7) McKean, D. R.; Schaedeli, U.; Kasai, P. H.; MacDonald, S. A. *Polym. Mater. Sci. Eng.* **1989**, *61*, 81.
(8) Allen, R. D.; Schaedeli, U.; McKean, D.; MacDonald, S. *Polym. Mater. Sci. Eng.* **1989**, *61*, 185.
(9) MacDonald, S. A.; Clecak, N. J.; Wendt, H. R.; Willson, C. G.; Snyder, C. D.; Knors, C. J.; Deyoe, N. B.; Maltabes, J. G.; Morrow, J. R.; McGuire, A. E.; Holmes, S. J. *SPIE Proc.: Adv. Resist Technol. Process. VIII* **1991**, *1466*, 2.
(10) Ban, H.; Deguchi, N. K.; Tanaka, A. *J. Vac. Sci.* **1991**, *B9*, 3387.
(11) Renner, C. U.S. Patent 4,371,605, 1983.

(12) O'Brien, M. *J. Polym. Eng. Sci.* **1989**, *29*, 846.
(13) Brunsvold, W.; Kwong, R.; Montgomery, W.; Moreau, W.; Sachdev, H.; Welsh, K. *SPIE Proc.: Adv. Resist Technol. Process. VII* **1990**, *1262*, 162.
(14) Brunsvold, W.; Montgomery, W.; Hwang, B. *SPIE Proc.: Adv. Resist Technol. Process. VIII* **1991**, *1466*, 368.
(15) Scruggs, B. E.; Gleason, K. K. *Macromolecules* **1992**, *25*, 1864.
(16) Yen, Y.-S.; Pines, A. *J. Chem. Phys.* **1983**, *78*, 3579.
(17) Baum, J.; Munowitz, M.; Garroway, A. N.; Pines, A. *J. Chem. Phys.* **1985**, *83*, 2015.
(18) Baum, J.; Pines, A. *J. Am. Chem. Soc.* **1986**, *108*, 7447.
(19) LaCelle, S. *Adv. Magn. Opt. Reson.* **1991**, *16*, 173.
(20) Scruggs, B. E.; Gleason, K. K. *J. Magn. Reson.* **1992**, *99*, 149.
(21) Munowitz, M. *Mol. Phys.* **1990**, *71*, 959.
(22) Scruggs, B. E.; Gleason, K. K. *Chem. Phys.* **1992**, *166*, 367.
(23) van Vleck, J. H. *Phys. Rev.* **1948**, *74*, 1168.
(24) Mehring, M. *Principles of High Resolution NMR in Solids*; Springer-Verlag: Berlin, 1983; pp 30–62.
(25) Slichter, C. P. *Principles of Magnetic Resonance*; Springer-Verlag: Berlin, 1978; p 36.
(26) Mehring, M.; Griffin, R. G.; Waugh, J. S. *J. Chem. Phys.* **1971**, *55*, 746.
(27) McKean, D. R.; Schaedeli, U.; MacDonald, S. A. *J. Polym. Sci., Polym. Chem. Ed.* **1989**, *27*, 3927.
(28) Baum, J.; Gleason, K. K.; Pines, A.; Garroway, A. N.; Reimer, J. A. *Phys. Rev. Lett.* **1986**, *56*, 1377.
(29) Hult, A.; MacDonald, S. A.; Willson, C. G. *Macromolecules* **1985**, *18*, 1804.
(30) Wang, L. F.; Pearce, E. M.; Kewi, T. K. *J. Polym. Sci. B* **1991**, *29*, 619.
(31) Brandrup, J., Immergut, E. H., Eds. *Polymer Handbook*, 3rd ed.; Wiley: New York, 1989; p VI/226.
(32) Belfiore, L. A.; Henrichs, P. M.; Cooper, S. L. *Polymer* **1984**, *25*, 452.
(33) Ngai, K. L.; Rendell, R. W.; Yee, A. F.; Plazek, D. J. *Macromolecules* **1991**, *24*, 61.
(34) Lui, Y.; Roy, A. K.; Jones, A. A.; Inglefield, P. T.; Ogden, P. *Macromolecules* **1990**, *23*, 968.
(35) Suvorava, A. I.; Hannonova, E. G. *Makromol. Chem.* **1990**, *191*, 993.